https://doi.org/10.2352/ISSN.2470-1173.2018.11.IMSE-457

Lag-Induced Image Artifacts in Still Imaging with CIS

Leo Anzagira[1], Orit Skorka, Pulla Reddy Ailuri[2], and Radu Ispasoiu
ON Semiconductor, San Jose, CA, USA
[1]Current Affiliation: Forza Silicon, Pasadena, CA, USA; [2]Current Affiliation: Intersil, Milpitas, CA, USA

Abstract

The most known impact of charge lag in image sensors is the phenomenon of "ghost images" which refer to the residual images created as a result of the trapped charge as the scene transitions from bright to dark. These "ghost" artifacts are particularly problematic for video imaging and, therefore, traditional lag characterization has focused on quantifying inter-frame charge smear. In still imaging, however, the impact of lag on image quality has not been thoroughly characterized. This work studies the effect of lag that is caused by photodiode-barrier on image quality in still imaging with CMOS image sensors. It shows a direct correlation between lag and fixed-pattern noise, demonstrates color artifacts that are caused by lag, and explains the mechanism that results in appearance of these artifacts.

Introduction

Advances in fabrication techniques and innovations in pixel and sensor design have led to improved CMOS image sensor performance and significant pixel miniaturization. As pixel sizes reach the 1 μm range, designers are faced with the problem of low full well capacity, which restricts the dynamic range. Although design optimization can often improve full well capacity, a common trade-off is increased image lag.

Image lag refers to the phenomenon where the presence or absence of charge in one frame impacts the recorded signal in this frame or in the subsequent frames. This can take the form of "charging lag" when imaging conditions change from dark to bright light and "discharging lag," when imaging conditions change from bright light to dark. Mechanisms responsible for image lag have been studied [1], [2]. Lag occurs when there is a potential barrier within the photodiode or along the charge transfer path of the pixel. Such potential barriers affect the recorded signal because they trap some of the charge. Figure 1 illustrates two possible sources of lag, one that is caused by a potential barrier that is formed inside the photodiode (PD), and one that is caused by a potential barrier at the transfer-gate (TX).

The well-known impact of lag is the phenomenon of "ghost images". It refers to the residual image artifact that is created as a result of the trapped charge as the scene transitions from bright to dark. These "ghost" artifacts are particularly problematic for video imaging and much effort has gone into reducing lag to minimize this artifact. Wang et al. [3] explain the correlation between fixed-pattern noise (FPN) of dark images, typically called dark signal non-uniformity (DSNU), and lag. However, to our knowledge, the impact of lag on image quality of still images has not been thoroughly studied. This work demonstrates and explains the effect of PD barrier lag in CMOS image sensors (CIS) on FPN of illuminated scenes and on color reproduction.

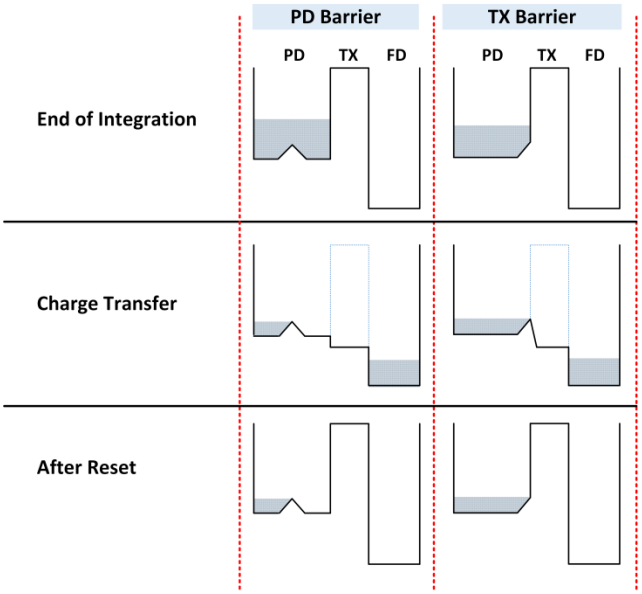

Figure 1 - Lag mechanisms showing the impact of potential barriers (a) in the photodiode (PD) and (b) at the edge of the transfer gate (TX). Both barriers result in lag as they prevent some of the electrons that are generated in the PD from being transferred to the floating diffusion (FD).

PD Barrier Lag Mechanism

This work focuses on the effect of lag on image quality with sensors that have a PD barrier. Gao et al. [4] explained that it is possible to distinguish between lag due to potential barrier at the edge of the TX or the FD and a potential barrier inside the PD as the edge-barrier lag varies with TX and FD voltages, whereas PD-barrier lag is insensitive to these voltages. In addition, PD-barrier lag is sensitive to idle time whereas edge-barrier lag is not. The term "idle time" is explained in the following paragraphs.

Figure 2 (a) presents the basic circuit diagram of a single 4T pixel in the array. At the beginning of an integration cycle, the reset (RST) transistor and the TX gate are turned on to reset the PD by enabling an electrical connection to the supply line, Vpix. Then, close to the end of the integration time, the RST transistor is turned ON to reset the FD capacitor. Charge that is accumulated in this capacitor is read as voltage by the source-follower (SF) transistor, which is not shown. The reset level is readout by activating the sample-and-hold-reset (SHR) control signal. Shortly after, the TX gate is turned ON to allow flow of charge from the PD to the FD and, after charge transfer is complete, the signal level is readout by activating the sample-and-hold-signal (SHS) control signal.

Frame time is the time interval between two consecutive PD reset operations; it represents the inverse of the video rate. Integration time is the time interval between a PD reset operation and the following charge transfer operation. To maintain a

specified video rate, it cannot exceed frame time, but it can be shorter. Idle time is defined as the time interval between charge transfer at the end of an integration time period within one frame and the PD reset signal that marks the beginning of the integration time period in the following frame.

If the pixel is operated with the longest possible integration time, as shown in Figure 2 (b), idle time is very short and only needed to allow digital signals to settle. For the purpose of this work, it is considered as 0. If integration time is shorter than frame time, as shown in Figure 2 (c), which may be needed to prevent saturation when exposure levels are high, the pixel spends a non-negligible amount of time in idle state in the time period between charge transfer and until the beginning of a new integration cycle.

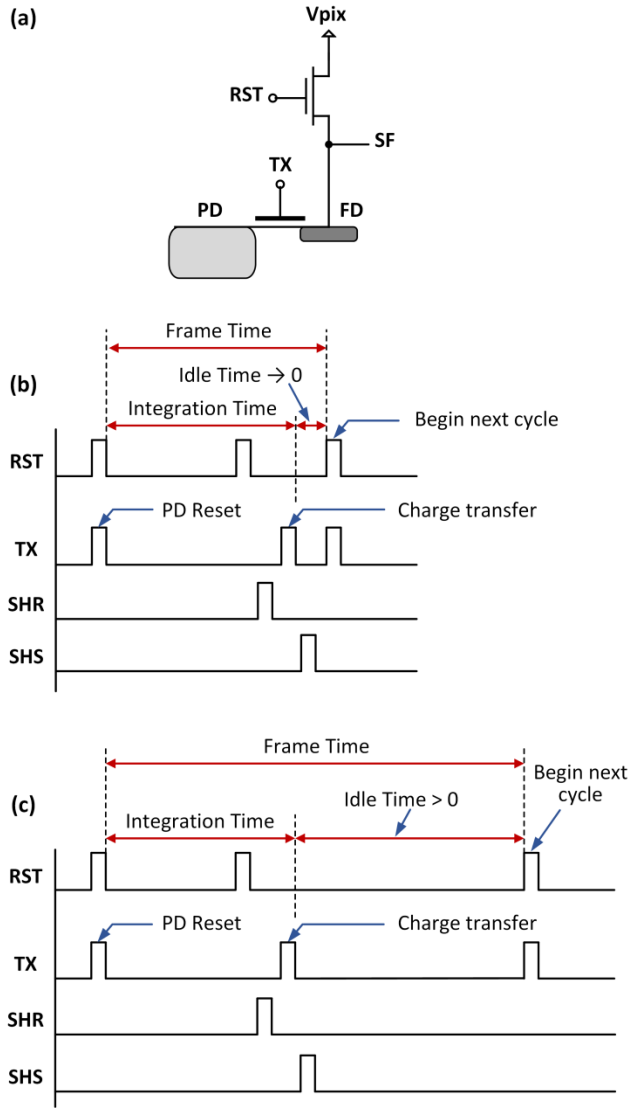

Figure 2 – Pixel timing and idle time. (a) The pixel circuit: Vpix is the pixel supply line, RST is the reset transistor, and SF is the output line that is connected to a source follower transistor; (b) When the pixel is operated with the longest possible integration time, a new integration cycle starts almost immediately after the charge from the previous cycle is transferred. Therefore, idle time is negligible and can be considered as 0; (c) When frame time is higher than integration time, there is a non-negligible time interval after charge transfer and before the beginning of a new integration cycle in which the pixel is idle.

In pixels with PD barrier, idle time impacts lag because charge, which is not transferred to the FD when TX is activated, can be emitted over the potential barrier by thermionic emission during idle time. The liberated charge carriers are cleared from the PD at the reset operation in the beginning of the next integration cycle. Therefore, with a long idle time, the level of lag that is measured can appear substantially lower than actual. This is illustrated in Figure 3.

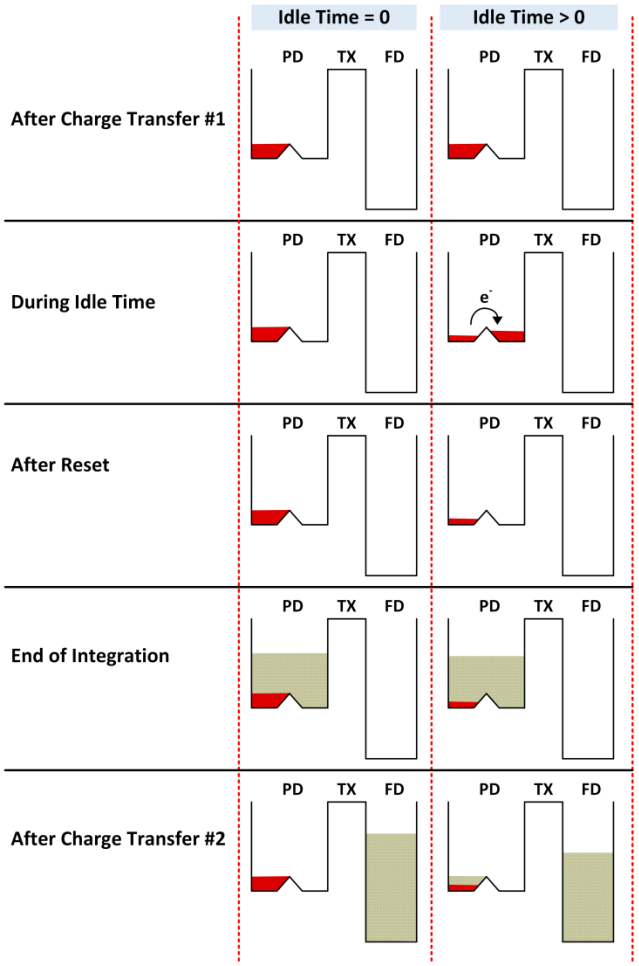

Figure 3 - Effect of idle time on lag in a pixel with PD barrier. If idle time >0, during idle time, some of the charge, which is left in the PD after charge transfer #1, flows over the potential barrier because of thermionic emission. Then, it is removed by the reset operation. Therefore, some of the charge that is accumulated in the PD during integration time is left in the PD after charge transfer #2. If there is no idle time (Idle Time = 0), although lag is higher, the effect of lag on performance is concealed.

The change in lag behavior with idle time can be leveraged to study the impact of lag on image quality. Even though long idle time appears to decrease the measured lag, this results in an almost empty PD charge pocket which has to be filled during each integration cycle. Pixel-to-pixel variations in PD barriers manifest in increased fixed pattern noise. Conversely, when there is no idle time, the measured lag appears higher, however, since charge pockets remain full at the beginning of the next integration cycle, they do not trap additional carriers during integration time. Furthermore, this may be considered as "lag free" functionality

because all the charge that is generated during integration time is transferred to the FD.

Lag Characterization

Lag was characterized using the pulsed light emitting diode (LED) method [4]. This method can be used to characterize both charging and discharging lag. To measure lag, the pulsed LED light source uniformly illuminates the sensor under test. Image capture sequence consists of a set of dark frames (LED light OFF) followed by a set of illuminated frames (LED light ON), followed by another set of dark frames (LED light OFF). A temporal mean is calculated for each frame in the dark, illuminated, dark frame sets.

To ensure reliable lag measurement, the rise and fall times of the pulsed LED must be significantly shorter than transient times of the image sensor. In addition, with rolling shutter sensors, one must also ensure that all rows are integrating during the period where the LED is ON. The charging lag can be determined from the difference between the first frame that is captured after the LED is turned ON and the last frame in the light frame set. The discharging lag can be determined from the difference between the first frame that is captured after the LED is turned OFF and the last frame in the dark frame set.

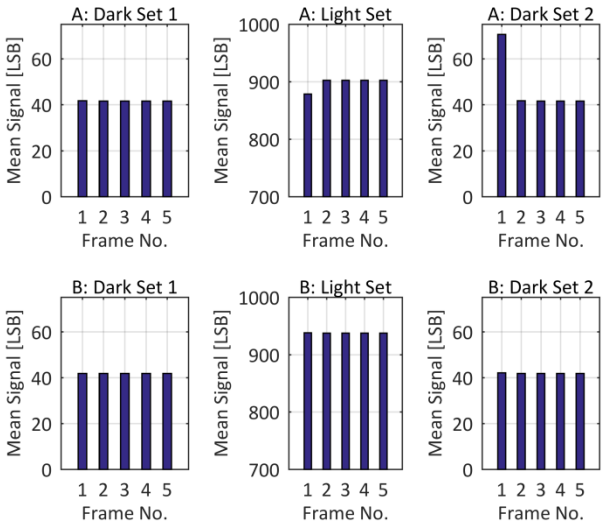

Figure 4 - Lag measurement on two sensors using the pulsed LED method. Sensor A, which has a PD barrier, exhibits charging and discharging lag, whereas Sensor B, which is a lag-free sensor, shows no lag.

In measuring lag, the sequence of frames may be captured in a standard sensor operation mode, in which case, the PD is reset after every capture. This may reduce the amount of lag measured since the reset operation cleans out some of the charge that remained from the previous frame. A more accurate measure of the lag can be obtained by disabling the reset operation between frames so that none of the trapped charge carriers from the previous frame are lost. Even though this mode of operation is not representative of the normal sensor operation mode, it does give a measure of the true level of lag and is useful for design improvement and sensor comparison.

This work presents experimental results that were obtained by comparing two 2.0 μm rolling shutter sensors with standard Bayer RGGB color filter array: Sensor A, which exhibits lag due to PD barrier, and Sensor B, which is a lag-free sensor. The peripheral circuits of the two sensors are identical; they include 10-bit analog-to-digital converters (ADCs) and their pedestal level is 42 LSB. Process and layout variations in the pixel fabrication process resulted in formation of a PD barrier in the pixels of Sensor A.

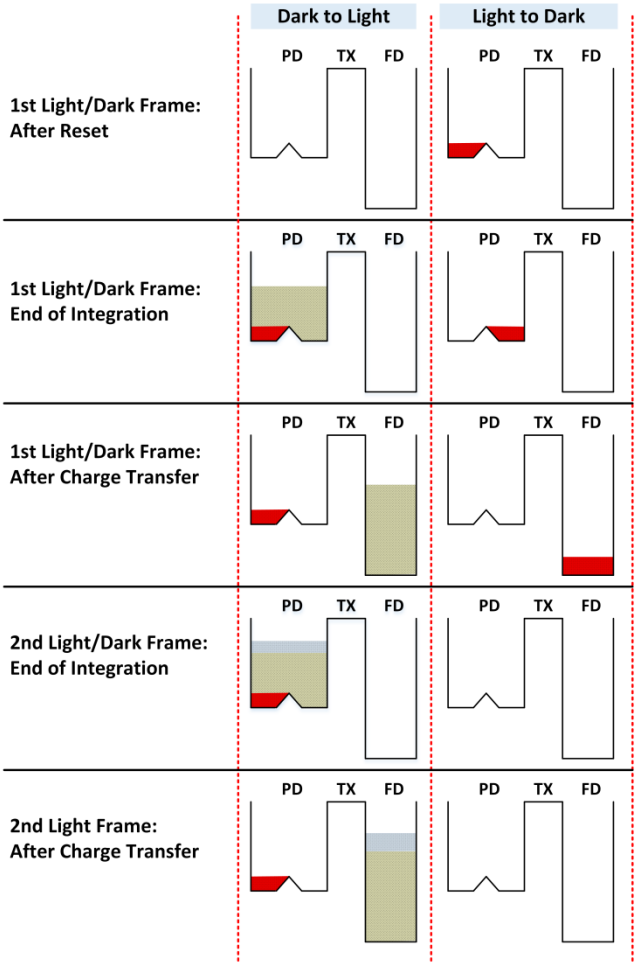

Figure 5 – In the transition from dark to light (left column), photo-generated charge that is trapped in the PD barrier results in charging lag. In the next frames, because all photo-generated charge is transferred to the FD, the "correct" signal level is obtained. In the transition from light to dark (right column), there is trapped charge in the PD at the beginning of the first frame. This charge is emitted over the potential barrier during integration time, where there is no photo-generation, and then it is transferred to the FD. This results in discharge lag. In the next frames, the PD remains empty and the "correct" dark level is obtained.

Figure 4 shows mean signal values of green pixels in the green-red row of the color filter array, Gr pixels, in Sensor A and Sensor B from the frame-sequence that was captured during a measurement with the pulsed LED method. Results are shown for a central region of 80×150 pixels in total, or 40×75 Gr pixels. A green LED was used for the measurement, and the pixels were activated with no idle time. The lag in sensor A is obvious from the first frame that is captured after light is turned ON and from the first frame that is captured after the light is turned OFF. The magnitude of the charging lag signal represents the amount of charge that is left in the PD after reset when the LED is ON. This is illustrated in the left column of Figure 5. The discharging lag

signal represents the amount of photo-generated charge that flows over the potential barrier during integration time, and then transferred to the FD after integration time ends. This is illustrated in the right column of Figure 5. Sensor B, on the other hand, shows no signature of lag as evidenced by the uniform signal level under similar illumination conditions.

To evaluate the impact of lag on FPN, each sensor was placed in a setup where the image plane could be uniformly illuminated with a green light source. The sensor was activated at a video rate of 14.5 fps and 30-frame data from a central region of 200×200 pixels were used for statistical analysis. Two data sets were collected from each sensor. With the first, integration time was set to 10 ms, which resulted in idle time of 57 ms and, with the second, there was no idle time. Light level was adjusted for each sensor and each data set to achieve a median signal level of 200 LSB.

Figure 6 shows signal histograms of Gr pixels in Sensors A and B. With Sensor A, one may observe a significant widening of the histogram when idle time is introduced. FPN, which represents the standard deviation in mean signal level in each data set, is higher in these conditions. While FPN for the case where there was no idle time is 1.6 LSB, FPN with idle time of 57 ms is 4.0 LSB. With Sensor B, on the other hand, there is no change in the histogram under both test conditions and, hence, there is no change in FPN. In both cases, FPN of Sensor B equals 1.6 LSB.

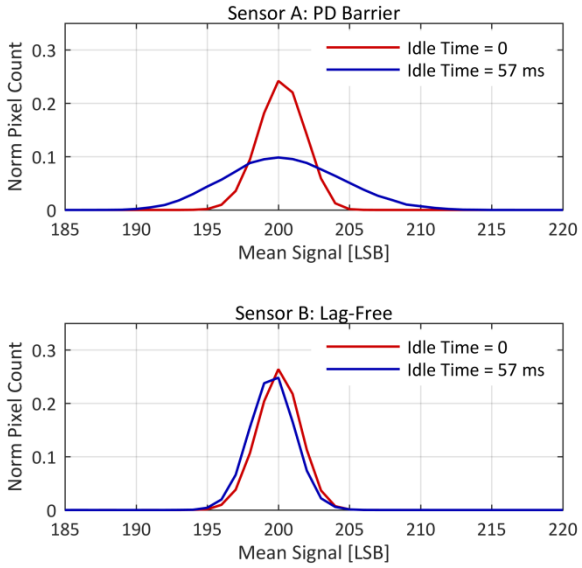

Figure 6 – Signal histograms of Sensor A and Sensor B for idle time of 0 and 57 ms. In all cases, median signal level is 200 LSB. However, while histogram shape remains almost unchanged in Sensor B when idle time is increased, it significantly widens in Sensor A.

Impact on image quality

To assess the impact of lag on image quality in still imaging, we compared images that were captured with Sensors A and B during operation with different idle times. The scene was illuminated with a 3,000K color temperature illuminant. Light intensity of the source was fixed and image plane illuminance was attenuated with metal-based neutral density filters that were placed in front of the camera to achieve the same mean signal level in both sensors for the same integration time. Signal level was measured in a uniform white central region of the resolution chart. This region of interest (ROI) is marked as ROI 1 in Figure 7 (a). The sensors were activated at video rate of 14.5 fps with analog gain of 1x. Focus adjustment was done manually. The camera module included a 670 nm interference infra-red cut filter and a Sunex DSL945D lens. The captured images were processed through a standard color processing pipeline that included white balancing, de-mosaic, color correction, and standard gamma correction. The pipeline, however, did not include correction for lens shading.

Figure 7 shows 30-frame average images that were captured with the two sensors with the longest possible integration time for the specified video rate to ensure that there is no idle time. The light was attenuated with neutral density filter ND0.3, and mean photo signal level in ROI 1 was about 675 LSB. Thirty individual frames were averaged in order to minimize the effect of temporal noise. Under these conditions, there are no noticeable differences between the images from Sensors A and B. This is consistent with FPN measurement results, which showed that the two sensors have comparable FPN when idle time is 0.

Figure 8 shows 30-frame average images that were captured under the exact same conditions that were used in Figure 7 but with no light attenuation in order to obtain high signal level with a shorter integration time. To maintain the same video rate, idle time here was 28 ms. Mean photo signal level in ROI 1 was about 705 LSB. When comparing the cropped images from Sensor A in Figure 7 (c) and Figure 8 (c), one may observe slight degradation in sharpness but, overall, differences are very subtle. There are no differences between the cropped images from Sensor B in Figure 7 (d) and Figure 8 (d).

Images of the same scene as captured with a neutral density filter ND1.0 and no idle time are presented in Figure 9. Mean photo signal level in ROI 1 was 127 LSB, which is about 13% of saturation level. Images from both sensors appear to have similar quality. Lastly, Figure 10 presents images that were captured without attenuation and with a shorter integration time to reach the same photo signal level of 127 LSB in ROI 1. Idle time here was greater than 60 ms.

By comparing the images in Figure 9 (a) and Figure 10 (a), which were captured with Sensor A, one may observe a substantial color shift that increases towards the peripheral regions of the image. White regions in the periphery of Figure 10 (a) appear to have brownish-yellowish color. No color shift is observed in neutral regions in the periphery of the corresponding images that were captured with Sensor B in Figure 9 (b) and Figure 10 (b). Comparison of the cropped images in Figure 9 (c) and Figure 10 (c) shows that the latter image is blurred and that it includes color noise. Both artifacts are directly related to the increase in fixed-pattern noise, where color noise is obtained after data from color pixels with fixed pattern noise is processed through the color pipeline.

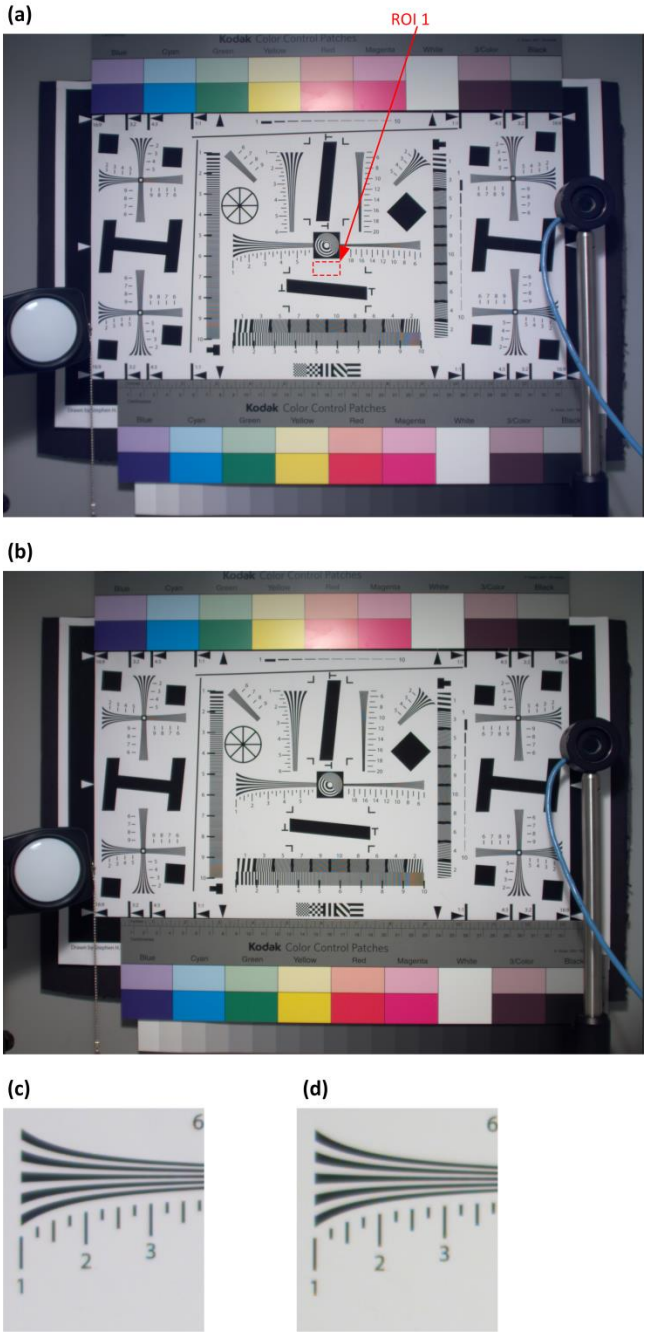

Figure 7 - Images (a) and (b) are 30-frame average images that were captured with Sensor A and Sensor B, respectively, with idle time = 0. The scene was illuminated with a warmlight illuminant, ~3,000K. Light level was attenuated with a ND0.3 filter to prevent saturation. Signal level of both sensors in the region that is marked as ROI 1 in (a) was similar. Images (c) and (d) were cropped from (a) and (b), respectively. There are no obvious image artifacts in either of the images.

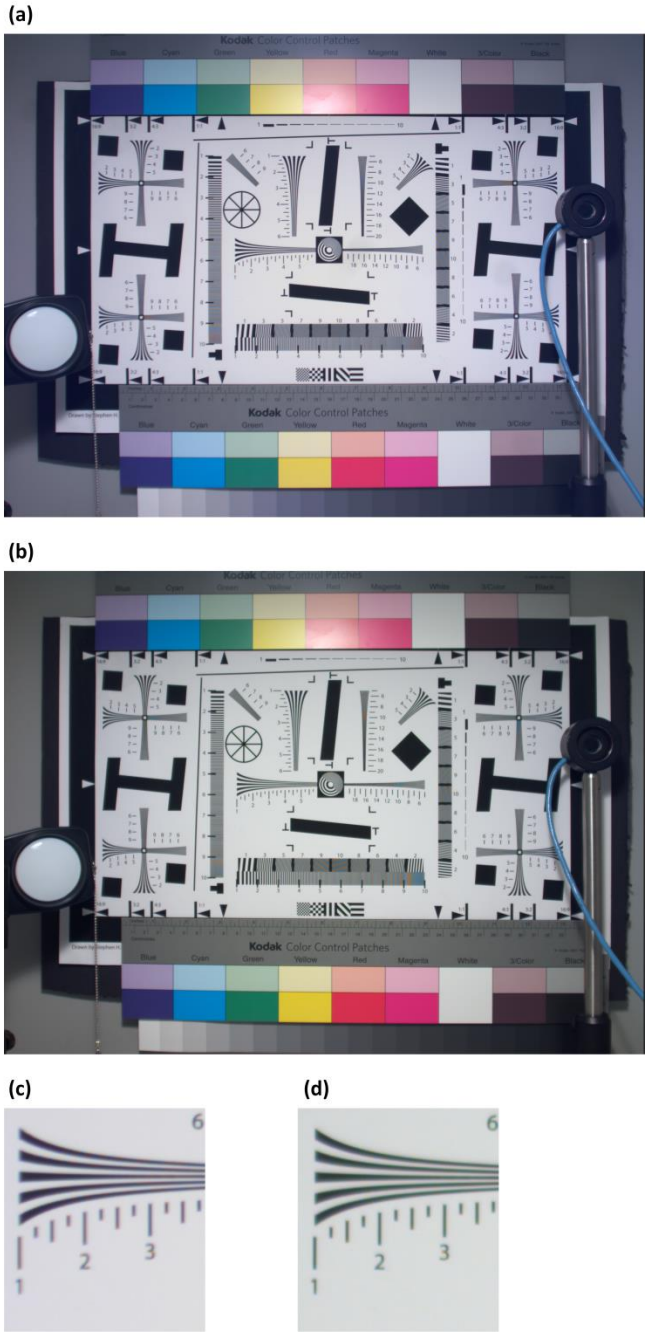

Figure 8 - Images (a) and (b) are 30-frame average images that were captured with Sensor A and Sensor B, respectively, with idle time = 28 ms. Images (c) and (d) were cropped from (a) and (b), respectively. The cropped image from Sensor A appears slightly less sharp than the one that was captured with the same sensor with idle time = 0, but differences are barely noticeable.

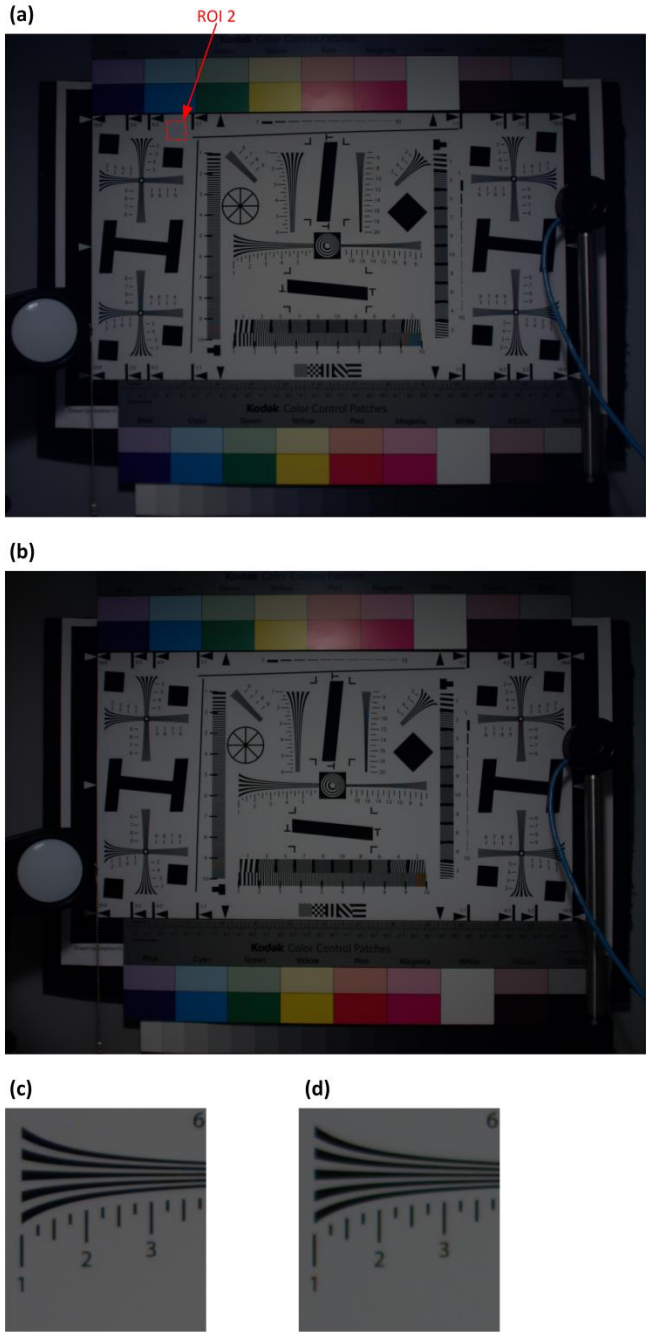

Figure 9 - Images (a) and (b) are 30-frame average images that were captured with Sensor A and Sensor B, respectively, with idle time = 0. Light level was attenuated with a ND1.0 filter to study the effect of low exposure on performance. Images (c) and (d) were cropped from (a) and (b), respectively. There are no obvious image artifacts in either of the images.

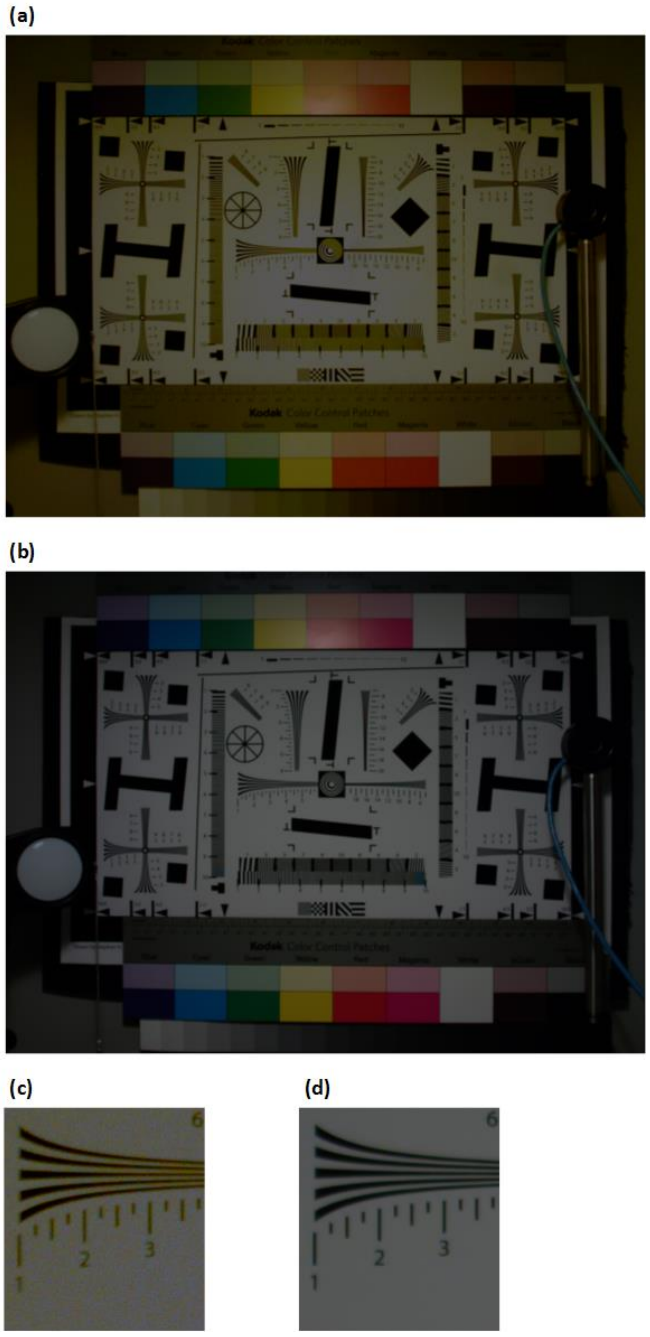

Figure 10 – Images (a) and (b) are 30-frame average images that were captured with Sensor A and Sensor B, respectively, with idle time > 60 ms. Illumination level was adjusted to achieve a similar mean signal level as in Figure 9 with integration time that is about an order of magnitude shorter. Images (c) and (d) were cropped from (a) and (b), respectively. The change in color towards yellow and the grainy texture can be easily observed in the images from Sensor A, which has PD-barrier lag.

To study the mechanism that leads to color shift, histograms of raw signal level after white-balance (10-bit data format) from all color planes in a peripheral region-of-interest, which is marked as ROI 2 in Figure 9 (a), were plotted for the images in Figure 9 (a) and Figure 10 (a). Results are presented in Figure 11 (a) and (b), respectively. Mean level of the blue channel signal is 3–4 LSBs higher than that of the red and green ones in Figure 11 (a) because the white balance coefficients were optimized for ROI 1, but lens-shading correction was not applied. One may observe that mean signal level of the blue channel is more than 20 LSB lower than that of the red and green ones in Figure 11 (b). The significant reduction in blue signal manifests in a region that is more dominant by green and red and this explains the shift in color towards yellow. The widening of the histograms in Figure 11 (b) (relative to Figure 11 (a)) is in agreement with the FPN test results, which were presented in Figure 6.

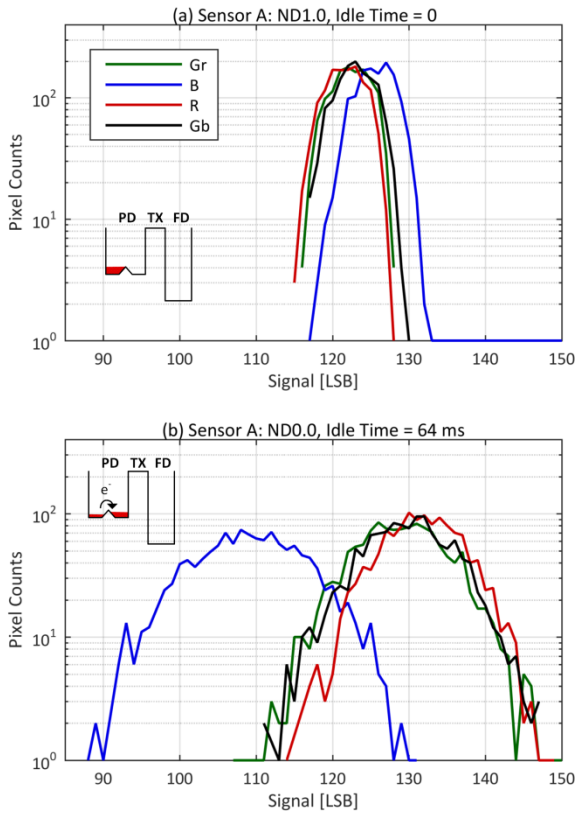

Figure 11 – Raw signal histogram (10-bit data format) of the four color planes after white balance in ROI 2 of (a) Figure 9 (a), and (b) Figure 10 (a). Median signal level of the blue channel is higher by 3–4 LSBs than that of the red and green channels in (a) due to the peripheral location of this ROI along with the fact that lens shading correction was not applied. Median signal level of the blue channel is lower by more than 20 LSBs in (b) because of the error that is introduced by the PD barrier and the thermionic emission mechanism during idle time and because of the warmlight illuminant, which has low intensity in the blue band on the spectrum.

The reason for the significant reduction in blue signal starts with the spectral composition of the warm light illuminant. This illuminant is rich in long wavelength photons but its intensity in the blue band is relatively low. Therefore, blue pixels receive fewer photons and produce less charge carriers than green and red pixels. The PD barrier and the thermionic emission mechanism during idle time introduce an error in the photo-charge that is transferred to the FD at the end of integration time. If exposure is high, as in Figure 8 (a), the error is low relative to the number of photo-generated charge carriers; therefore, there is no clear change in hue. However, if exposure is low, as in Figure 10 (a), there is an obvious change in color. Figure 12 illustrates the two cases.

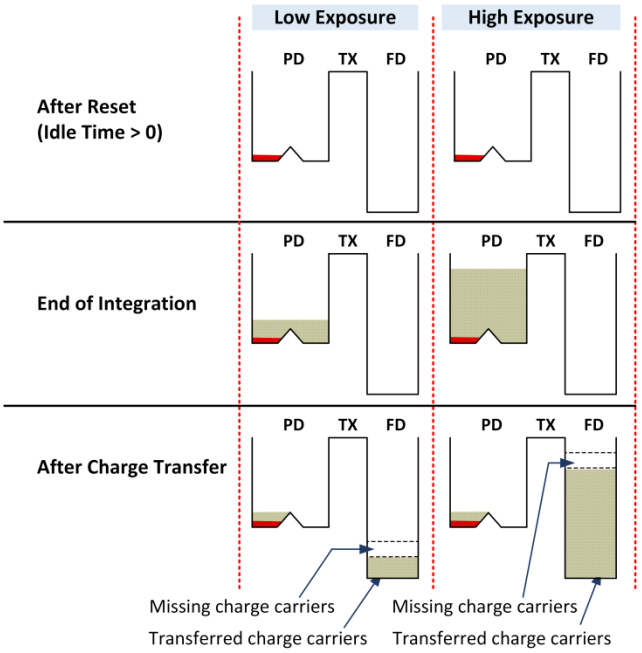

Figure 12 – Illustration of the dynamics of photo-generated charge-carriers in Sensor A, which has a PD barrier, when activated with a long idle time under low and high exposure conditions. In both cases, there is loss of charge-carriers in steady exposure. However, when the number of charge carriers is low to begin with, the error is more significant and this can result in change in color.

Conclusion

This work studied the effect of PD-barrier lag on image quality in still imaging. It showed that thermionic emission has a major role in the effect of this type of lag on image quality. In low light conditions, performance with PD-barrier lag is sensitive to idle time, which is the time interval during which the sensor is not integrating photo-charge. With a long idle time, there is an increase in fixed-pattern noise, which is directly related to degradation in spatial resolution. In color sensors, color noise and color shift are likely to appear after processing through a standard pipeline. Under steady illumination conditions, PD-barrier lag can be concealed if these sensors are activated when the pixels are constantly integrating. When there is no idle time, image quality of sensors with PD-barrier lag is similar to that of lag-free sensors with a similar pixel design.

Works Cited

[1] E. R. Fossum, "Charge Transfer Noise and Lag in CMOS Active Pixel Sensors," *IEEE Workshop on Charge-Coupled Devices and Advanced Image Sensors,* pp. 1-6, 2003.

[2] L. E. Bonjour, N. Blanc and M. Kayal, "Experimental Analysis of Lag Sources in Pinned Photodiodes," *IEEE Electron Device Letters,* vol. 33, no. 12, pp. 1735-1737, 2012.

[3] X. Wang, P. R. Rao and A. J. Theuwissen, "Fixed-Pattern Noise Induced by Transmission Gate in," *IEEE European Solid-State Device Research Conference,* pp. 331-334, 2006.

[4] W. Gao, M. Guidash, N. Li, R. Ispasoiu, P. R. Ailuri, N. Palaniappan, D. Tekleab and M. Rahman, "Photodiode Barrier Induced Lag Characterization Using a New Lag versus Idle Time Methodology," *International Image Sensors Workshop,* pp. 1-4, 2017.

Author Biography

Leo Anzagira received his BA and BE degrees from Dartmouth College in 2011 and his PhD from the Thayer Engineering school at Dartmouth in 2016. He subsequently joined the Pixel and Sensor Characterization team at ON Semiconductor Corp. He is now a product engineer at Forza Silicon Corporation.

Orit Skorka received her BSc from Ben-Gurion University of the Negev, Israel, in 2001, her MSc from the Technion IIT, Israel, in 2004, and her Ph.D. from the University of Alberta, Canada, in 2011, all in Electrical and Computer Engineering. She joined Aptina in 2013 and is now with the Image Sensor Group at ON Semiconductor working on pixel characterization and image quality of CMOS image sensors for mobile imaging and automotive applications.

Pulla R. Ailuri received his BS in Electronics and Communication Engineering from Osmania University, India, in 2005, and his MS in Electrical Engineering from New Mexico State University, USA, in 2008. His MS research work focused on dynamic current mirror active pixel image sensors. He joined Aptina in 2009 as a Product Engineer, and became a Pixel Characterization Engineer in 2013. Since July 2017 he is working on Optical Sensors as an Applications Engineer at Intersil Corporation.

Radu Ispasoiu is a senior manager of pixel R&D and image quality at ON Semiconductor ISG (since 2014). He has held engineering management and lead R&D positions in the Silicon Valley optoelectronics technology industry for more than 17 years. He holds a PhD in Physics (1996) with focus on semiconductor optoelectronic device study from the University of Oxford, UK.